THE JOURNAL OF BIOLOGICAL CHEMISTRY VOL. 285, NO. 25, pp. 19227–19234, June 18, 2010

Conditional Ablation of the Heparan Sulfate-synthesizing Enzyme *Ext1* Leads to Dysregulation of Bone Morphogenic Protein Signaling and Severe Skeletal Defects*[S]

Received for publication, January 20, 2010, and in revised form, March 24, 2010 Published, JBC Papers in Press, April 19, 2010, DOI 10.1074/jbc.M110.105338

Yoshihiro Matsumoto[‡1], Kazu Matsumoto[‡1], Fumitoshi Irie[‡], Jun-ichi Fukushi[§], William B. Stallcup[§], and Yu Yamaguchi[‡2]

From the [‡]Sanford Children's Health Research Center and [§]Cancer Center, Sanford-Burnham Medical Research Institute, La Jolla, California 92037

Increasing evidence indicates that heparan sulfate (HS) is an integral component of many morphogen signaling pathways. However, its mechanisms of action appear to be diverse, depending on the type of morphogen and the developmental contexts. To define the function of HS in skeletal development, we conditionally ablated *Ext1*, which encodes an essential glycosyltransferase for HS synthesis, in limb bud mesenchyme using the *Prx1-Cre* transgene. These conditional *Ext1* mutant mice display severe limb skeletal defects, including shortened and malformed limb bones, oligodactyly, and fusion of joints. In developing limb buds of mutant mice, chondrogenic differentiation of mesenchymal condensations is delayed and impaired, whereas the area of differentiation is diffusely expanded. Correspondingly, the distribution of both bone morphogenic protein (BMP) signaling domains and BMP2 immunoreactivity in the mutant limb mesenchyme is broadened and diffuse. In micromass cultures, chondrogenic differentiation of mutant chondrocytes is delayed, and the responsiveness to exogenous BMPs is attenuated. Moreover, the segregation of the pSmad1/5/8-expressing chondrocytes and fibronectin-expressing perichondrium-like cells surrounding chondrocyte nodules is disrupted in mutant micromass cultures. Together, our results show that HS is essential for patterning of limb skeletal elements and that BMP signaling is one of the major targets for the regulatory role of HS in this developmental context.

Endochondral ossification, one of the two major modes of bone formation, is responsible for the formation of limb bones (1, 2). Within developing limb buds, mesenchymal progenitor cells form condensations, in which chondrocytes and perichondrial cells differentiate in the core and in the periphery, respectively. Hypertrophic chondrocytes direct perichondrial cell differentiation into osteoblasts, whereas perichondrial cell signaling regulates proliferation and hypertrophic changes in chondrocytes. These differentiation processes are governed by an intricate signaling network involving secreted morphogens and growth factors, including bone morphogenic proteins (BMPs),[3] fibroblast growth factors, Indian hedgehog (Ihh), parathyroid hormone-related hormone, and WNT proteins (1, 3).

Heparan sulfate proteoglycans (HSPGs) play critical roles in many developmental processes. Many growth factors and morphogens, including those that play a role in skeletal development, exhibit affinities for the heparan sulfate (HS) chains of HSPGs (4, 5). The physiological importance of HS in skeletal development is also illustrated by the presence of a human bone disorder caused by genetic defects in enzymes involved in HS synthesis. Multiple hereditary exostoses (MHE) is an autosomal dominant disorder characterized by the formation of multiple osteochondromas as well as by limb bone deformity and is caused by hemizygous mutation of *Ext1*, which encodes a glycosyltransferase essential for HS synthesis (6, 7). Mutations of *Ext2*, which encodes an EXT1-related protein that forms heterodimers with EXT1, also cause MHE.

To determine the molecular mechanism of HS action in skeletal development, we ablated HS synthesis in the limb skeletal system using the conditional $Ext1^{flox}$ allele (8) and the *Prx1-Cre* transgene (9). Phenotypic analysis of conditional *Ext1* mutants and *in vitro* experiments using *Ext1*-deficient mesenchymal cells reveal that HS is essential for normal development of the limb skeleton, especially in the context of the development and patterning of mesenchymal condensations. Our result suggests that BMP signaling is one of the focal points of HS involvement in this developmental process.

EXPERIMENTAL PROCEDURES

Mice—Conditional *Ext1* mutant mice were generated by crossing the $Ext1^{flox}$ allele (8) and the *Prx1-Cre* transgene (9). Littermates that inherited the incomplete combination of the above alleles were used as wild-type controls. All experiments were done with mice in complete C57BL/6 background. All protocols for animal use were approved by the IACUC of the Burnham Institute for Medical Research and were in accordance with National Institutes of Health guidelines.

Skeletal Analysis—For whole-mount analysis of skeletons, mice were eviscerated and fixed in 95% ethanol overnight. The

* This work was supported, in whole or in part, by National Institutes of Health Grants R01 AR055670 (to Y. Y.), R01 CA95238 (to W. B. S.), and P01 HD25938 (to Y. Y. and W. B. S.). This work was also supported by the MHE Coalition and the MHE Research Foundation.

[S] The on-line version of this article (available at http://www.jbc.org) contains supplemental Figs. 1–3.

[1] Both authors contributed equally to this work.

[2] To whom correspondence should be addressed: Sanford-Burnham Medical Research Institute, 10901 North Torrey Pines Rd., La Jolla, CA 92037. Tel.: 858-646-3124; Fax: 858-795-5387; E-mail: yyamaguchi@burnham.org.

[3] The abbreviations used are: BMP, bone morphogenic protein; HS, heparan sulfate; HSPG, heparan sulfate proteoglycan; MHE, multiple hereditary exostoses.

preparations were stained with Alcian blue for 24 h, rinsed in 95% ethanol, incubated 2% KOH for 12 h, and stained with Alizarin red for 24 h. The stained preparations were cleaned in 20% glycerol, 1% KOH for 5 days and transferred to 50% glycerol, 50% ethanol for photography and storage.

Histological Analyses—Embryos were fixed in 4% paraformaldehyde in phosphate-buffered saline, washed in phosphate-buffered saline, and embedded in OCT compound. Frozen sections of these specimens were stained with Alcian blue and counterstained with nuclear fast red. For immunohistochemistry, cryosections were blocked with 5% goat serum and incubated overnight at 4 °C with the following primary antibodies: the anti-HS antibody 10E4 (Seikagaku, Tokyo, Japan); anti-phospho-Smad1/5/8 polyclonal antibody (Cell Signaling Technology, Beverly, MA); anti-fibronectin monoclonal antibody (BD Biosciences); and anti-type II collagen polyclonal antibody (Research Diagnostics, Concord, MA). After incubation with primary antibodies, sections were incubated with Alexa fluor 488- or Alexa fluor 568-conjugated secondary antibodies (Invitrogen), followed by counterstaining with 4′,6-diamidino-2-phenylindole dihydrochloride (Invitrogen). For staining with the anti-HS antibody 10E4 (Seikagaku, Tokyo, Japan), cryosections were fixed with acetone, blocked with 10% goat serum, incubated with the antibody overnight at 4 °C, and visualized with Cy2-conjugated goat anti-mouse IgM (Jackson ImmunoResearch). For the analysis of BMP2 in limb buds, tissues were fixed with Saint Marie's solution (10). Whole-mount and section *in situ* hybridization analyses were performed as described previously (8) with the following RNA probes: *Ext1* (8); *Col2a1* (11); *Sox9* (from Dr. Véronique Lefebvre) (12); *Hoxd11* and *Hoxd13* (from Dr. Clifford Tabin) (13); *Fgf8* (from Dr. Gail Martin) (14); *Hoxd12* and *Hoxa13* (from Dr. J. C. Belmonte) (15); and *Shh* (from Dr. R. Kip Guy) (16).

Micromass Cultures—Limb buds from E11.5 embryos were dissected, and cells were dissociated by incubation in Puck's solution A (0.4 mg/ml KCl, 8 mg/ml NaCl, 0.35 mg/ml $NaHCO_3$, 1 mg/ml glucose) containing 10 mg/ml dispase and 10% chick serum for 1.5 h at 37 °C (17). Ten μl of dissociated cell suspension (2×10^7 cells/ml) were plated on a 4-well tissue culture dish. Cells were allowed to adhere for 1 h at 37 °C in a humidified CO_2 incubator and then fed with 0.5 ml of Dulbecco's modified Eagle's medium/F-12 (mixed at a ratio of 2:3) containing 10% fetal bovine serum. Cultures were incubated up to 6 days with medium changes every 2nd day. Alcian blue staining and immunostaining of micromass cultures were performed as described previously (18).

Image Analysis—Chondrogenic differentiation of micromass cultures was analyzed by Alcian blue staining. The area occupied by Alcian blue$^+$ nodules was quantified by using ImageJ software (version 1.36b) on images acquired under identical exposure and lighting conditions, as described previously (18). The integrated optical density of representative dishes was quantified by reversing the bright and dark regions of grayscale images of cultures and determining the average grayscale value (on a scale of 0–256) using ImageJ software, as described previously (18).

Real Time Quantitative PCR—Total RNA was extracted using TRIzol reagent (Invitrogen) from E11.5 limb buds (for *Ext1*; Fig. 1) or micromass cultures (for *Bmp2* and *Bmp4*; Fig. 5). One μg of total RNA was reverse-transcribed using the Superscript III first-strand synthesis system (Invitrogen). SYBR Green-based quantitative real time PCR analysis was carried out using the Stratagene Mx3000p sequence detection system (Applied Biosystems). The expression level of each target gene was calculated by standardizing the target gene copy number with the glyceraldehyde-3-phosphate dehydrogenase copy number in a sample. The analysis of the results is based on duplicate samples from four independent experiments. The primer sequences were as follows: *Ext1*, 5′-GCCCTTTT-GTTTTATTTTGG-3′ and 5′-TCTTGCCTTTGTAGAT-GCTC-3′; *Bmp2*, 5′-TGCACCAAGATGAACACAG-3′ and 5′-GCTGTTTGTGTTTGGCTTG-3′; *Bmp4*, 5′-GGACTTC-GAGGCGACACTTC-3′ and 5′-GCCGGTAAAGATCCCT-CATG-3′; *Gapdh*, 5′-CCAGTATGACTCCACTCACG-3′ and 5′-GACTCCACGACATACTCAGC-3′.

RESULTS

Ablation of Ext1 in Limb Bud Mesenchyme Causes Severe Skeletal Defects—*Ext1* was conditionally ablated using the *Prx1-Cre* transgene, which drives recombination in the limb bud mesenchyme starting at E9.5 (9, 19). Ablation of *Ext1* expression and HS production in limb bud mesenchyme was verified by quantitative reverse transcription-PCR, immunohistochemistry, and immunoblotting for HSPG glycosylation. Quantitative reverse transcription-PCR showed an ~90% reduction in the level of *Ext1* mRNA in mutant E11.5 limb buds (supplemental Fig. 1*A*). The residual *Ext1* mRNA is likely derived from its expression in the ectoderm, because *Prx1-Cre* is not activated in the limb bud ectoderm (9). Consistently, we found that HS immunoreactivity is preserved in the ectoderm (supplemental Fig. 1*B*). Immunoblotting analysis revealed that syndecan-3, one of the abundantly expressed HSPGs in the developing limb, is expressed as a naked core protein (supplemental Fig. 1*C*), further confirming efficient inactivation of HS synthetic activity. Whole-mount *in situ* hybridization showed that expression patterns of other genes involved in early limb bud patterning are not noticeably altered in *Prx1-Cre;Ext1$^{flox/flox}$* embryos (supplemental Fig. 2).

Conditional *Ext1* homozygous mutants (*Prx1-Cre; Ext1$^{flox/flox}$*) were born alive at the expected Mendelian ratio but die within 6 h of birth. The exact cause of death of *Prx1-Cre; Ext1$^{flox/flox}$* mice is not clear, but it may be related to the fact that these mutants display hypoplastic limbs (Fig. 1*A*, *mt*) and are immobile due to the agenesis of limb joints (see below). Conditional heterozygous mutants (*Prx1-Cre;Ext1$^{flox/+}$*) were viable with no detectable abnormalities (data not shown). Skeletal preparations of E18.5 mutant embryos revealed severe abnormalities in the limb skeleton (Fig. 1*B*). The long bones of *Prx1-Cre;Ext1$^{flox/flox}$* mutants were shortened to about one-third the length of those in wild-type littermates, although the width was increased (Fig. 1*B*, *FL*). In the elbow, the humerus was fused with the radius and ulna by continuous ossification (Fig. 1*B*, *EJ*). The humerus and scapula were joined by continuous cartilaginous elements without the presence of a joint (Fig. 1*B*, *SJ*). The number of digits in mutants ranged from 2 to 5, with many carpal and metacarpal bones either missing or fused

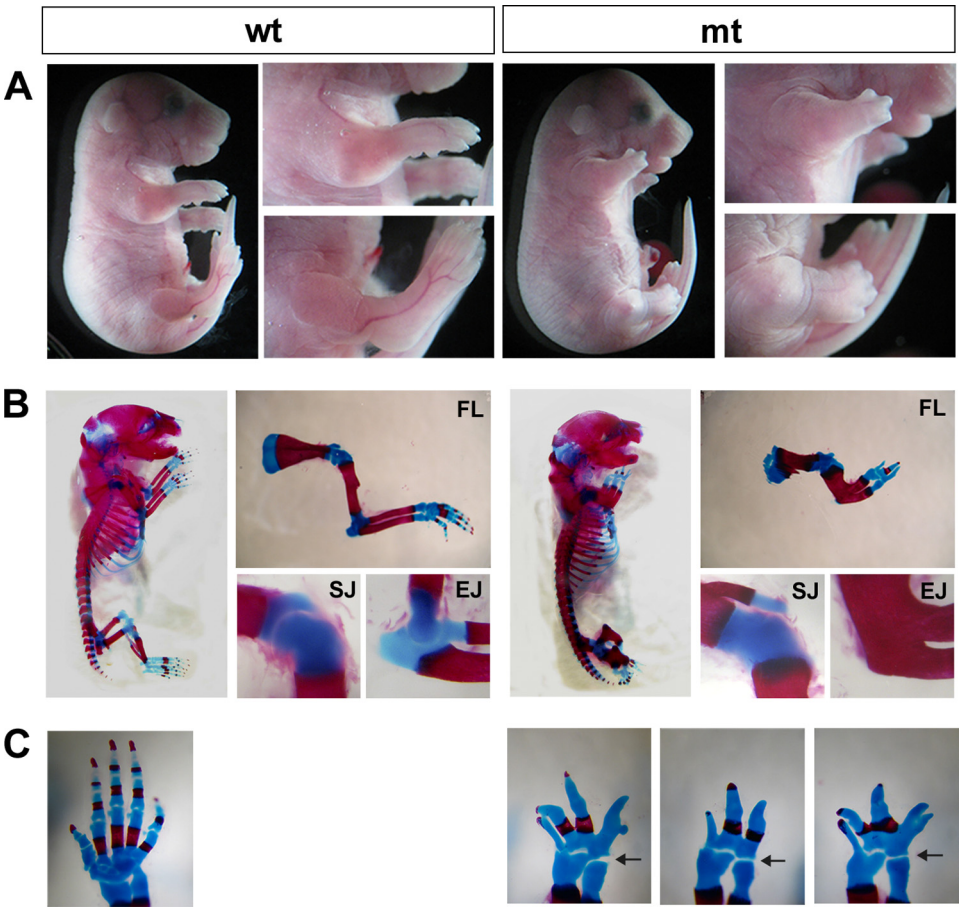

FIGURE 1. **Skeletal phenotypes of conditional *Ext1* mutants.** *Prx1-Cre;Ext1*$^{flox/flox}$ (*mt*) and wild-type (*wt*) littermates are shown. More than 12 animals for each genotype were examined for these analyses. *A,* gross morphology at E18.5. Note that mutants have severely shortened forelimbs and hindlimbs. *B,* Alcian blue/Alizarin red-stained skeletal preparations at P0. Close-up views of the forelimb (*FL*), shoulder joint (*SJ*), and elbow joint (*EJ*) are also shown. *C,* defects in autopod skeletal elements. Forepaws of a wild-type (*wt*) and three *Prx1-Cre;Ext1*$^{flox/flox}$ (*mt*) mice at P0 are shown. Note that there are variable numbers of digits in mutant mice (see also Table 1). All joints in the autopod are fused, although the wrist joint (*arrows*) was preserved in all *Prx1-Cre;Ext1*$^{flox/flox}$ mice examined.

TABLE 1
Summary of forelimb phenotypes of *Prx1-Cre;Ext1*$^{flox/flox}$ mice

Structure	Phenotype	Occurrence (penetrance)
Scapula	Shortened and broadened	12/12 (100%)
Humerus	Shortened and broadened	12/12 (100%)
Radius/ulna	Shortened and broadened	12/12 (100%)
Carpal bones	Fused	12/12 (100%)
Metacarpal bones	Not identifiable	12/12 (100%)
Phalanges	Abnormal phalanges	12/12 (100%)
	Oligodactyly	11/12 (92%)
	No. of phalanges	
	1	0/12
	2	1/12
	3	6/12
	4	4/12
	5	1/12
Shoulder joint	Absent (fused with cartilage)	12/12 (100%)
Elbow joint	Absent (fused with continuous ossification)	12/12 (100%)
Wrist joint	Present	12/12 (100%)
Digit joints	Absent	12/12 (100%)

together (Fig. 1*C*, *mt*). All of the above phenotypes were observed with essentially 100% penetrance (Table 1). Overall, the phenotype of *Prx1-Cre;Ext1*$^{flox/flox}$ mutants is much more penetrant and severe than that of mice homozygous for the gene-trapped *Ext1*^{Gt} allele (20), indicating a role for HS in limb skeletal development that is more extensive than that deduced from hypomorphic *Ext1*$^{Gt/Gt}$ mutants.

Development of Limb Abnormalities in Ext1 Mutant Mice—Examination of earlier mutant embryos revealed that patterning and growth of condensations are already abnormal at E12.5. In mutants, chondrogenesis of distal skeletal elements was delayed, although the cartilage template of the humerus was short and broad (Fig. 2*B*). At E14.5, all stylopod and zeugopod cartilage templates in mutants were shortened, and there was no indication of the development of correctly patterned digits. Failure of joint formation was apparent in the shoulder and elbow of mutants at E14.5 (Fig. 2*D*; compare with wild-type shown in Fig. 2*C*). At E16.5, ossification occurred both in wild-type and mutant mice, but in mutants, the humerus, radius, and ulna ossified as a continuous bone (Fig. 2*F*). The phenotype at this stage was essentially the same as that seen at P0 (see Fig. 1*B*). These results demonstrate that the basis for the skeletal defects observed in newborn mutant mice is already present as early as E12.5. This confirms roles for HS in early phases of limb skeletal development before Ihh becomes a major factor in skeletal development (21).

To investigate the molecular basis of these limb phenotypes, forelimb sections were analyzed by *in situ* hybridization. At E11.5, *Sox9* and *Col2a1* were both expressed in mutant limbs at intensities similar to those in wild-type mice (Fig. 2, *G–J*), indicating that the program for chondrogenic differentiation is initiated relatively normally in mutants. However, the spatial patterns of *Sox9* and *Col2a1* expression in mutants were altered; both *Sox9* and *Col2a1* expression domains were enlarged in mutants (Fig. 2, *H* and *J*). At E12.5, *Col2a1* expression levels in wild-type mice increased greatly, and *Col2a1* expression domains were separated into multiple subdomains corresponding to individual cartilage templates (Fig. 2*K*). In contrast, *Col2* expression in mutant mice was diffuse, lacking distinct subdomains (Fig. 2*L*).

Aberrant Development and Differentiation of Mesenchymal Condensations in Ext1 Mutant Mice—The foregoing results suggest that the phenotypes of *Prx1-Cre;Ext1*$^{flox/flox}$ mutants originate primarily from abnormal growth and differentiation of cartilage condensations. Therefore, we focused on determining some of the basic defects in cartilage condensations in the mutant mice. At E12.5, both wild-type and mutant limbs con-

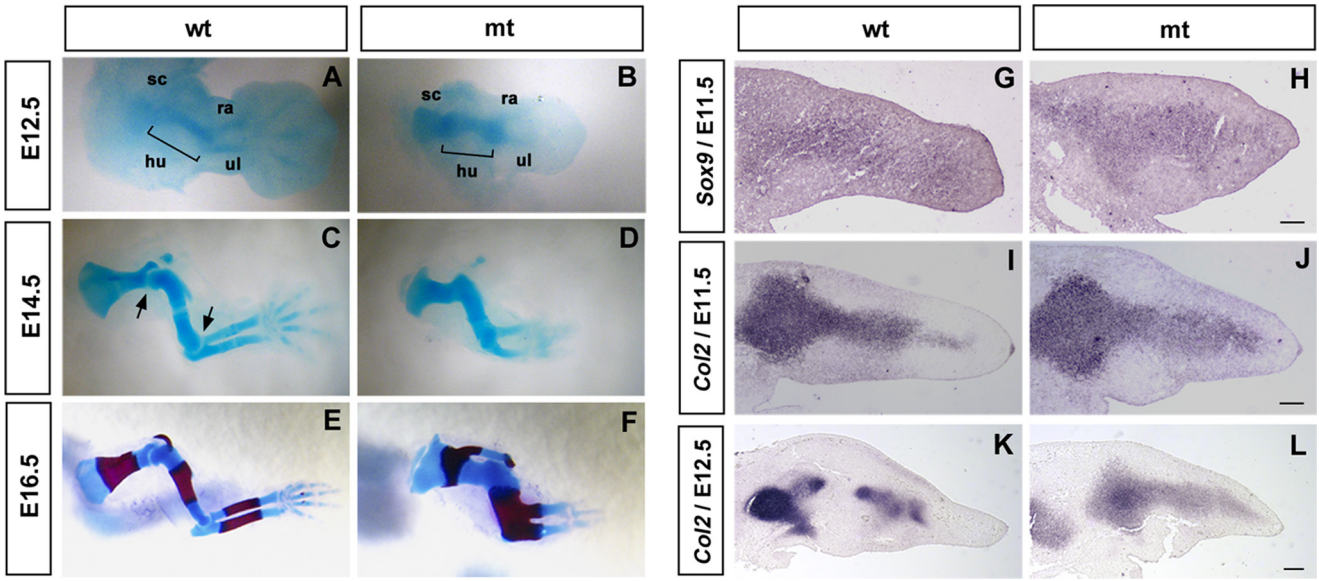

FIGURE 2. **Analysis of the development of skeletal phenotypes in conditional *Ext1* mutants.** *A–F*, development of the forelimb skeleton in wild-type (*wt*) and *Prx1-Cre;Ext1*$^{flox/flox}$ (*mt*) embryos. Forelimbs of E12.5, E14.5, and E16.5 embryos are stained with Alcian blue. E16.5 specimens are also stained with Alizarin red. *sc*, scapula; *hu*, humerus; *ra*, radius, *ul*, ulna. In mutant mice, abnormal patterning and shape of cartilage templates are apparent as early as E12.5 (*B*). *G–L*, molecular analysis. Sections of E11.5 and E12.5 forelimbs were analyzed for *Sox9* and *Col2a1*. Although the early chondrocyte markers *Sox9* and *Col2a1* are expressed rather normally at E11.5, up-regulation and spatial restriction of *Col2a1* expression seen in wild-type limbs at E12.5 do not occur in mutants (*L*). *Scale bar*, 100 μm.

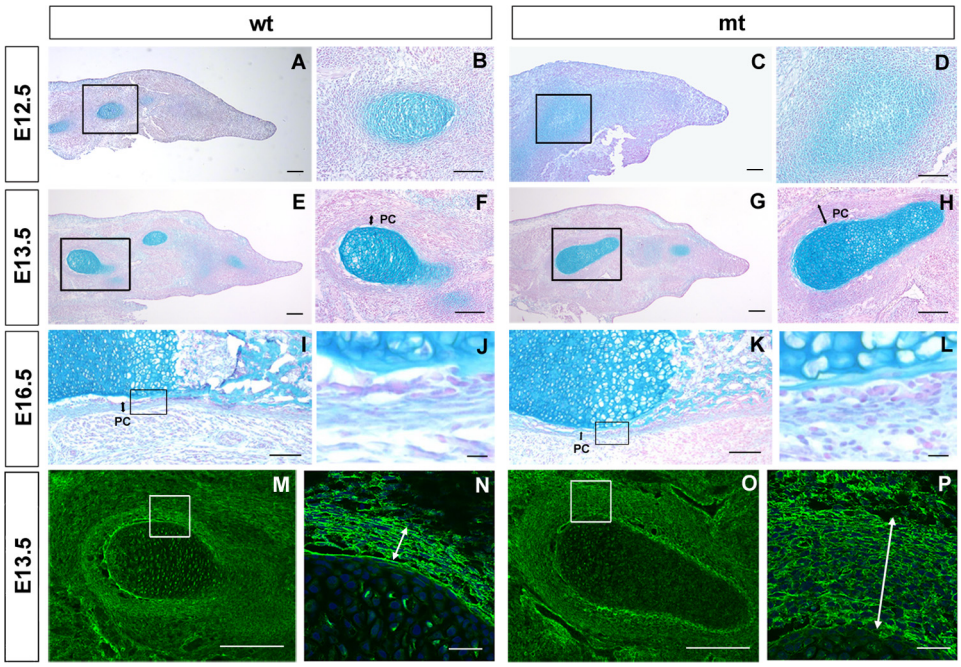

FIGURE 3. **Growth and differentiation of cartilage condensations in conditional *Ext1* mutants.** *A–L*, limb bud sections of wild-type (*wt*) and *Prx1-Cre;Ext1*$^{flox/flox}$ (*mt*) embryos were stained with Alcian blue and Nuclear Fast Red. *A–D*, E12.5; *E–H*, E13.5; *I–L*, E16.5. Note delayed chondrocyte differentiation (*C* and *D*) and abnormal perichondrium (*H* and *L*) in mutant condensations. *M–P*, E13.5 limb bud sections were immunostained for fibronectin. *Scale bar*, 100 μm for *A, C, E, G, M*, and *O*; 50 μm for *B, D, F*, and *H*; 10 μm for *J, L, N*, and *P*. *Boxed areas* are shown at a higher magnification to the *right*. Perichondrial layers are indicated by *double arrows*.

tained Alcian blue-stained condensations (Fig. 3, *A* and *C*). However, in mutants, the intensity of staining was weak, and the area of Alcian blue staining was diffusely expanded (Fig. 3*D*). Weakened Alcian blue staining in mutants is not the consequence of the loss of tissue HS due to *Ext1* ablation, because Alcian blue staining predominantly reflects the amount of chondroitin sulfate; chondroitinase treatment of limb sections eliminated essentially all Alcian blue staining, whereas heparitinase treatment had little effect (supplemental Fig. 3*A*). At E13.5, mutant cartilage templates continued to exhibit abnormal morphology and patterning (Fig. 3, *G* and *H*). On the other hand, the intensity of staining was now largely equivalent to that of wild-type mice, indicating that *Ext1*-deficient mesenchymal cells are capable of undergoing chondrogenic differentiation, albeit delayed.

Prx1-Cre;Ext1$^{flox/flox}$ mice also display abnormalities in perichondrial development. In wild-type mice, presumptive perichondrial cells began to flatten and align as a concentric layer surrounding the condensation at E12.5 (Fig. 3*B*). These morphological changes were not apparent in mutants (Fig. 3*D*). At E13.5, wild-type mice exhibited a well defined perichondrium composed of flattened cells that stain positively for fibronectin (Fig. 3, *M* and *N*). In mutant mice, the perichondrium-like layer was more than three times as thick as that of wild-type mice, and the perichondrial cells had a less flattened morphology (Fig. 3, *H* and *P*). At E16.5, thinning of the mutant perichondrium was equivalent to that of the wild type, but the shape of individual perichondrial cells was rounder, and the outer boundary of the perichondrium was unclear (compare Fig. 3, *J* and *L*).

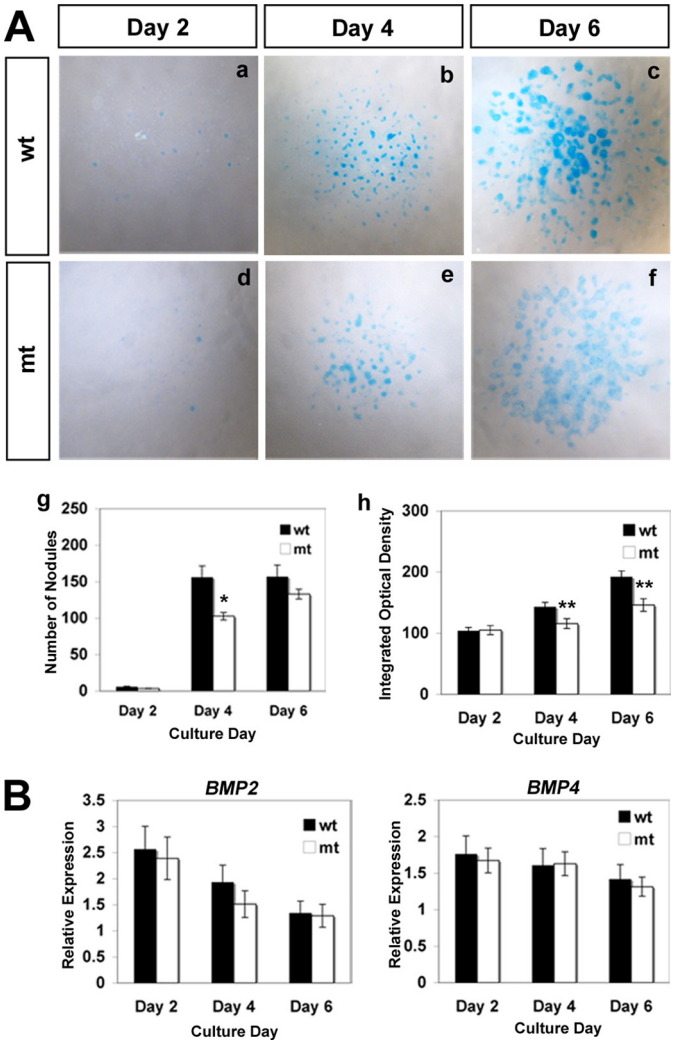

FIGURE 4. **Chondrogenic differentiation of *Ext1*-deficient limb bud mesenchyme in micromass cultures.** *A*, impaired differentiation of *Ext1*-deficient mesenchymal cells in micromass culture. *Panels a–f*, micromass cultures derived from E11.5 wild-type (*wt*), and *Prx1-Cre;Ext1*$^{flox/flox}$ (*mt*) embryos were stained with Alcian blue after indicated days of incubation. *Panel g*, number of Alcian blue^{+} nodules. Data represent the means ± S.D. of the number of nodules per culture. The number of cultures analyzed = 4. *, $p < 0.05$. *Panel h*, intensity of Alcian blue staining in nodules. Data represent the means ± S.D. of integrated optical density (see "Experimental Procedures"). The number of nodules analyzed (pooled from four independent cultures) = 20 (day 2), 50 (day 4), and 50 (day 6). **, $p < 0.01$. *B*, quantitative reverse transcription-PCR analysis of *Bmp2* and *Bmp4* mRNA expression in micromass cultures. Data represent the means ± S.D. of the relative expression level. The number of RNA samples analyzed = 4 (isolated from independent cultures). There are no statistically significant differences at any time points.

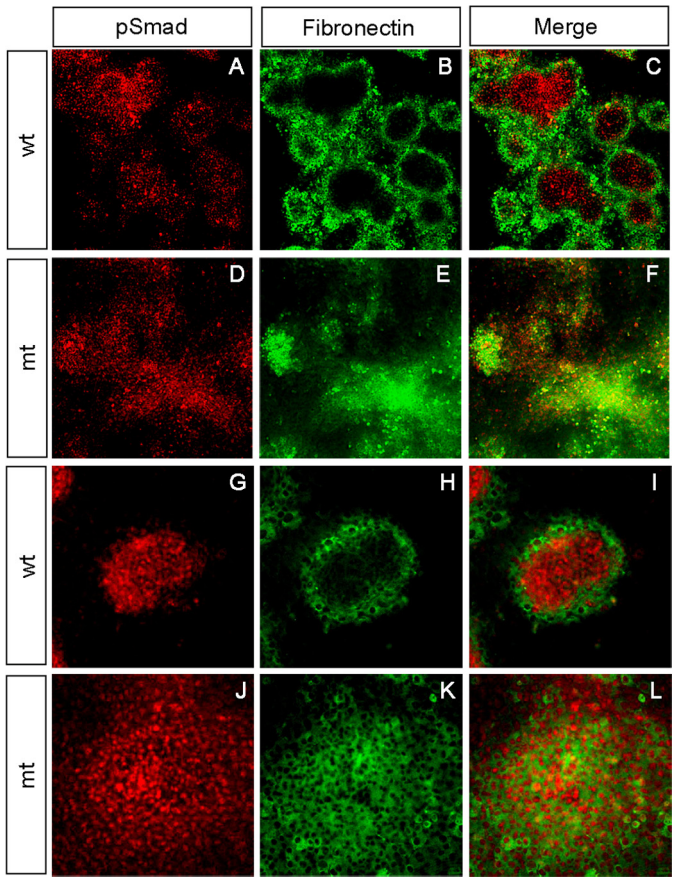

FIGURE 5. **Abnormal BMP signaling and perichondrial differentiation in *Ext1*-deficient micromass cultures.** Micromass cultures from E11.5 wild-type (*wt*) and *Prx1-Cre;Ext1*$^{flox/flox}$ embryos cultured for 4 days and double-stained with anti-pSmad and anti-fibronectin antibodies. *A–F*, low magnification views of micromass cultures. *G–L*, high magnification views of single cartilage nodules. Note that cartilage nodules derived from wild-type mesenchyme exhibit clear segregation of pSmad^{+} central core and fibronectin^{+} perichondria-like cells (*C* and *I*). In contrast, cartilage nodules from mutant (*mt*) cells fail to undergo segregation (*F* and *L*), and pSmad^{+} cells and fibronectin^{+} cells are intermixed within the nodule (*L*). The experiments were repeated four times using independent embryos with similar results.

Chondrogenic Differentiation of Ext1-deficient Mesenchymal Cells in Vitro—To gain mechanistic insight into the aberrant development of chondrogenic condensations in mutant mice, we performed *in vitro* analyses using micromass cultures. In wild-type cultures, robust chondrogenesis occurred over the course of 6 days in culture (Fig. 4*A*). Although chondrogenesis did occur in mutant cultures, it was less robust and delayed compared with wild-type cultures (Fig. 4*A*, *panels d–f* and *panels g* and *h*). Again, the reduced Alcian blue staining seen in mutant cultures is not attributed to the loss of HS in mutant cultures (supplemental Fig. 3*B*). These changes are not due to the impairment of endogenous BMP expression in mutant cells, as mutant and wild-type cells express similar levels of *Bmp2* and *Bmp4* mRNA (Fig. 4*B*).

Among several HS-binding morphogens and growth factors, BMPs play a central role in the formation of chondrogenic condensations (22–24), and BMPs bind HS (25–27). To examine the status of BMP signaling in mutant chondrocytes, we examined micromass cultures by immunostaining with anti-phospho-Smad-1, -5, and -8 (pSmad1/5/8) and anti-fibronectin antibodies to analyze BMP signaling and perichondrial differentiation, respectively (Fig. 5). In wild-type cultures, cartilage nodules were of spheroidal shape with pSmad1/5/8-expressing chondrocytes forming a compact core and fibronectin-expressing perichondrium-like cells surrounding the core (Fig. 5, *G–I*). pSmad1/5/8-expressing and fibronectin-expressing domains were well segregated with little intermixing of the two cell types (Fig. 5, *C* and *I*). Mutant chondrocytes exhibited comparable levels of pSmad1/5/8 immunoreactivity (Fig. 5*D*), indicating that *Ext1*-deficient cells can transduce BMP signals. However, the segregation of the pSmad1/5/8-expressing chondrocytes and fibronectin-expressing perichondrium-like cells was

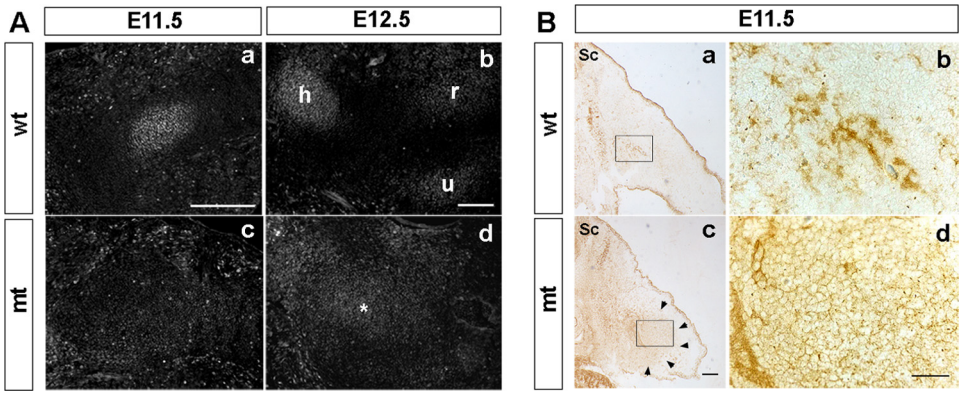

FIGURE 6. **Spatial range of BMP signaling and localization of BMP2 protein *in vivo*.** *A,* BMP signaling domains in limb buds. Sections of the forelimbs from wild-type (*wt*) and *Prx1-Cre;Ext1*$^{flox/flox}$ (*mt*) embryos at E11.5 and E12.5 were stained with anti-pSmad1/5/8 antibody. In E11.5 wild-type limb buds, pSmad1/5/8 expression coincides with mesenchymal condensations (*panel a*), whereas no such discrete pSmad expression domains were found in mutant limb buds (*panel c*). At E12.5, mutant limb buds contain a single broad pSmad1/5/8^{+} domain that shows weak staining (*asterisk* in *panel d*), whereas wild-type limb buds show separate pSmad1/5/8^{+} domains that correspond to individual cartilage condensations (*panel b*). *h,* humerus; *r,* radius; *u,* ulna. *B,* distribution of BMP2 protein in the limb buds. Sections of the forelimb buds from E11.5 wild-type (*panels a* and *b*) and *Prx1-Cre;Ext1*$^{flox/flox}$ (*panels c* and *d*) embryos were stained with anti-BMP2 antibody. *Top* is dorsal; *left* is medial. *Sc,* spinal cord. *Boxed areas* in *panels a* and *c* are shown at a higher magnification in *panels b* and *d*, respectively. Note the broad distribution of BMP2 immunoreactivity in mutants (its spatial extent is indicated by *arrowheads* in *panel c*). Intercellular BMP immunoreactivity extends well into surrounding mesenchymal tissues in mutants (*panel d*). Representative results from three independent embryos are shown. *Scale bar,* 100 μm.

totally disrupted in mutant cultures. pSmad1/5/8-expressing cells were distributed broadly without forming discrete cores (Fig. 5*F*). Nodules also contain fibronectin-expressing cells intermixed with pSmad1/5/8-expressing chondrocytes (Fig. 5, *J–L*). Together, these results demonstrate that, although *Ext1*-deficient cells are capable of transducing BMP signals, the tight spatial regulation of BMP signaling observed in wild-type cartilage condensations is disrupted in the absence of HS.

Loss of HS Expression Alters Spatial Range of BMP Signaling and Localization of BMP2 Protein in Vivo—To obtain *in vivo* evidence corroborating the foregoing observation, we examined BMP signaling activity and the distribution of BMP proteins in limb buds of mutant mice. In wild-type mice, discrete domains of pSmad1/5/8 immunoreactivity were detected, coinciding with developing condensations (Fig. 6*A*, *panels a* and *b*). In contrast, no discrete domains of pSmad1/5/8 immunoreactivity were observed within mutant limbs at E11.5 (Fig. 6*A*, *panel c*). At E12.5, pSmad1/5/8 immunoreactivity became detectable in mutants, but its distribution was more diffuse than in wild-type mice (Fig. 6*A*, *panel d*).

One of the possible reasons for the diffuse BMP signaling domain in mutant limbs is that BMP protein may also distribute diffusely in the absence of HS. Thus we examined by immunohistochemistry the distribution of endogenous BMP2 proteins within the limb bud tissues. In wild-type mice, BMP2 immunoreactivity was observed in a highly concentrated manner (Fig. 6*B, panels a* and *b*). In contrast, BMP2 immunoreactivity in the mutant mesenchyme displayed a diffuse distribution (Fig. 6*B, panel c*, indicated by *arrowheads*). Interestingly, it is clear under high magnification that intercellular BMP2 immunoreactivity extends broadly into surrounding mesenchymal tissues (Fig. 6*B, panel d*). No such intercellular staining was observed in wild-type mesenchyme (Fig. 6*B, panel b*). These results suggest that BMP2 diffuses more freely in the absence of HS.

DISCUSSION

In this study, we report the use of the conditional *Ext1* null allele and the *Prx1-Cre* transgene to determine the role of HS in skeletal development. The phenotype of conditional *Ext1* mutants was significantly different from that of mice homozygous for the gene-trapped *Ext1*^{Gt} allele (20), especially in terms of the penetrance and expressivity of phenotypes. The variable expressivity and incomplete penetrance of phenotypes in *Ext1*$^{Gt/Gt}$ mutants are likely attributable to alternative splicing around the insertion site (28). In contrast, *Prx1-Cre;Ext1*$^{flox/flox}$ mutants invariably survive until birth, exhibiting complete penetrance and consistent expressivity of skeletal phenotypes (see Table 1). These features of the conditional *Ext1* ablation model reveal that the role of HS in skeletal development is more extensive than that deduced from the analysis of *Ext1*$^{Gt/Gt}$ mutants. Our data indicate that at least three aspects of limb skeletal development require normal expression of HS, namely development of mesenchymal condensations, patterning of digits, and joint development. Considering the known role of HS in morphogen binding, it is likely that the absence of HS disrupts some aspect(s) of morphogen signaling that is critical for each of these developmental processes.

Our phenotypic analysis suggests that abnormal patterning and development of mesenchymal condensations provide the primary basis for the severely shortened and malformed limb bones of *Prx1-Cre;Ext1*$^{flox/flox}$ mice. It has been shown that BMP signaling plays a major role in the development of mesenchymal condensations (22, 24, 29–31). Our analyses with the anti-pSmad1/5/8 antibody indicate that the robustness and spatial range of BMP signaling in developing condensations is indeed compromised in the absence of HS, demonstrating the physiological importance of HS in BMP function during this developmental process.

To further understand the physiological importance of HS in BMP signaling, it is of interest to compare the phenotype of *Ext1* mutant mice with those of other mutant mice. Notably, the phenotypes of mice with mutations in several other morphogenic signaling pathways, including the fibroblast growth factor, Ihh, Wnt, and vascular endothelial growth factor pathways, are distinct from that of *Prx1-Cre;Ext1*$^{flox/flox}$ mice (21, 32–36). In contrast, mice with mutations in the BMP pathway share interesting phenotypic similarities with *Prx1-Cre;Ext1*$^{flox/flox}$ mice, especially in terms of the development of condensations. Conditional knock-out of two of the BMP receptor genes, *Bmpr1a* and *Bmpr1b*, almost completely inhibits chondrogenic differentiation of condensations (24). The level of

inhibition of chondrogenesis and the resulting skeletal phenotype of these *Bmpr1a*/*Bmpr1b* compound mutant mice are much more severe than that of *Prx1-Cre;Ext1*$^{flox/flox}$ mice. On the other hand, chondrogenesis proceeds with a slight delay even in the absence of *Bmp2* and *Bmp4*, the two major BMP species expressed in the developing limb skeletal elements (37). This phenotype of *Bmp2/Bmp4* compound mutants resembles that of *Prx1-Cre;Ext1*$^{flox/flox}$ mice, in which chondrogenesis is also delayed but eventually achieved (see Fig. 3). On the other hand, *Bmp2/Bmp4* compound mutants are not reported to have the abnormal condensation morphology observed in *Prx1-Cre;Ext1*$^{flox/flox}$ mice. It is somewhat surprising that the absence of both BMP2 and BMP4 does not produce a more severe phenotype than the absence of HS. This may be due to the action of other BMPs, such as BMP5, BMP6, and BMP7 (37). Such a scenario would also suggest that the regulatory role of HS extends to multiple BMP species. Another possibility that cannot be entirely ruled out is that the condensation phenotype of *Prx1-Cre;Ext1*$^{flox/flox}$ mice includes the effect of HS elimination on signaling pathway(s) other than the BMP pathway.

HS is thought to regulate signaling by a number of HS-binding morphogens and growth factors by diverse, but not mutually exclusive, mechanisms. In the cases of FGF2 and netrin-1, HS acts as an essential coreceptor, for ligand interaction with the cognate receptors that activate downstream signaling (38, 39). Our analysis of mutant limb buds and micromass cultures revealed that the intensity of BMP signaling is somewhat impaired, but not entirely abolished, in the absence of HS. These results are not consistent with the model in which HS acts as an obligatory coreceptor for BMPs. Rather, our results suggest that HS simply sequesters BMPs within and in close proximity to condensations without the necessity of HS interaction with cognate receptors for the ligands. This mechanism could serve to maintain high concentrations of BMPs near the cell surface to provide sustained, high intensity signals in developing tissues. The diffuse and weakened chondrogenesis of mutant condensations is likely to be due to the increased diffusion of BMPs in the absence of HS.

One of the limitations of this study is that it does not allow precise dissection of the direct effect of HS on BMPs from indirect effects through Noggin, one of the BMP antagonists, which also binds HS (40). It is noteworthy, however, that there is no indication, from either our *in vivo* or *in vitro* results, that BMP signaling is enhanced in the absence of HS. This observation does not appear to be consistent with the model that HS is required for BMP antagonism by Noggin, because loss of HS should reduce this antagonism.

Although our results indicate that regulation of BMP signaling is an important role of HS during early skeletal development, the phenotype of *Prx1-Cre;Ext1*$^{flox/flox}$ mice suggests additional HS targets. First, a severe autopod phenotype suggests that HS plays a critical role in digit patterning. It is conceivable that cross-talk between the ectoderm and mesenchyme during the early phase of limb bud patterning, which is mediated by the HS-binding morphogens Shh and FGF4 (41), is also physiologically regulated by HS. Second, the agenesis of joints suggests a pervasive role for HS in the signaling events that control joint formation. Wnt/catenin signaling, known to play a pivotal role in specifying joints (42, 43), is a likely target of HS in this process, because Wnt proteins are bound to and modulated by HS (44, 45).

Although HS deficiency due to mutation of *Ext1* (or *Ext2*) is undoubtedly the primary cause of MHE, the molecular mechanism leading to the formation of osteochondromas remains elusive. In this vein, it is interesting to note that patients with fibrodysplasia ossificans progressiva, which is caused by constitutively activating mutations in the BMP receptor AVCR1, often develop multiple osteochondromas that resemble those in MHE (46). This observation resonates with our present finding that the BMP signaling pathway is a major target of the regulatory function of HS during skeletal development. Dysregulation of BMP signaling may be a mechanism of osteochondroma formation in MHE. Further analyses of *Ext1* conditional knock-out mice may shed light on the molecular mechanism of MHE pathogenesis.

Acknowledgments—We thank Drs. J. C. Belmonte, R. K. Guy, V. Lefebvre, G. Martin, A. McMahon, A. Oohira, and C. Tabin for providing reagents. Ext1^{flox} *mice were generated in collaboration with Lexicon Genetics.*

REFERENCES

1. Kronenberg, H. M. (2003) *Nature* **423,** 332–336
2. Olsen, B. R., Reginato, A. M., and Wang, W. (2000) *Annu. Rev. Cell Dev. Biol.* **16,** 191–220
3. Colnot, C. (2005) *J. Cell. Biochem.* **95,** 688–697
4. Bishop, J. R., Schuksz, M., and Esko, J. D. (2007) *Nature* **446,** 1030–1037
5. Kreuger, J., Spillmann, D., Li, J. P., and Lindahl, U. (2006) *J. Cell Biol.* **174,** 323–327
6. Duncan, G., McCormick, C., and Tufaro, F. (2001) *J. Clin. Invest.* **108,** 511–516
7. Zak, B. M., Crawford, B. E., and Esko, J. D. (2002) *Biochim. Biophys. Acta* **1573,** 346–355
8. Inatani, M., Irie, F., Plump, A. S., Tessier-Lavigne, M., and Yamaguchi, Y. (2003) *Science* **302,** 1044–1046
9. Logan, M., Martin, J. F., Nagy, A., Lobe, C., Olson, E. N., and Tabin, C. J. (2002) *Genesis* **33,** 77–80
10. Gritli-Linde, A., Lewis, P., McMahon, A. P., and Linde, A. (2001) *Dev. Biol.* **236,** 364–386
11. Fukushi, J., Inatani, M., Yamaguchi, Y., and Stallcup, W. B. (2003) *Dev. Dyn.* **228,** 143–148
12. Lefebvre, V., Garofalo, S., and de Crombrugghe, B. (1995) *J. Cell Biol.* **128,** 239–245
13. Burke, A. C., Nelson, C. E., Morgan, B. A., and Tabin, C. (1995) *Development* **121,** 333–346
14. Sun, X., Mariani, F. V., and Martin, G. R. (2002) *Nature* **418,** 501–508
15. van der Hoeven, F., Sordino, P., Fraudeau, N., Izpisúa-Belmonte, J. C., and Duboule, D. (1996) *Mech. Dev.* **54,** 9–21
16. Guy, R. K. (2000) *Proc. Natl. Acad. Sci. U.S.A.* **97,** 7307–7312
17. James, C. G., Appleton, C. T., Ulici, V., Underhill, T. M., and Beier, F. (2005) *Mol. Biol. Cell* **16,** 5316–5333
18. Fisher, M. C., Li, Y., Seghatoleslami, M. R., Dealy, C. N., and Kosher, R. A. (2006) *Matrix Biol.* **25,** 27–39
19. Selever, J., Liu, W., Lu, M. F., Behringer, R. R., and Martin, J. F. (2004) *Dev. Biol.* **276,** 268–279
20. Koziel, L., Kunath, M., Kelly, O. G., and Vortkamp, A. (2004) *Dev. Cell* **6,** 801–813
21. St-Jacques, B., Hammerschmidt, M., and McMahon, A. P. (1999) *Genes Dev.* **13,** 2072–2086
22. Brunet, L. J., McMahon, J. A., McMahon, A. P., and Harland, R. M. (1998) *Science* **280,** 1455–1457

23. Pizette, S., and Niswander, L. (2000) *Dev. Biol.* **219,** 237–249
24. Yoon, B. S., Ovchinnikov, D. A., Yoshii, I., Mishina, Y., Behringer, R. R., and Lyons, K. M. (2005) *Proc. Natl. Acad. Sci. U.S.A.* **102,** 5062–5067
25. Ruppert, R., Hoffmann, E., and Sebald, W. (1996) *Eur. J. Biochem.* **237,** 295–302
26. Ohkawara, B., Iemura, S., ten Dijke, P., and Ueno, N. (2002) *Curr. Biol.* **12,** 205–209
27. Irie, A., Habuchi, H., Kimata, K., and Sanai, Y. (2003) *Biochem. Biophys. Res. Commun.* **308,** 858–865
28. Stanford, W. L., Cohn, J. B., and Cordes, S. P. (2001) *Nat. Rev. Genet.* **2,** 756–768
29. Hall, B. K., and Miyake, T. (2000) *BioEssays* **22,** 138–147
30. Duprez, D., Bell, E. J., Richardson, M. K., Archer, C. W., Wolpert, L., Brickell, P. M., and Francis-West, P. H. (1996) *Mech. Dev.* **57,** 145–157
31. Macias, D., Gañan, Y., Sampath, T. K., Piedra, M. E., Ros, M. A., and Hurle, J. M. (1997) *Development* **124,** 1109–1117
32. Li, C., Xu, X., Nelson, D. K., Williams, T., Kuehn, M. R., and Deng, C. X. (2005) *Development* **132,** 4755–4764
33. Verheyden, J. M., Lewandoski, M., Deng, C., Harfe, B. D., and Sun, X. (2005) *Development* **132,** 4235–4245
34. Yu, K., Xu, J., Liu, Z., Sosic, D., Shao, J., Olson, E. N., Towler, D. A., and Ornitz, D. M. (2003) *Development* **130,** 3063–3074
35. Hill, T. P., Später, D., Taketo, M. M., Birchmeier, W., and Hartmann, C. (2005) *Dev. Cell* **8,** 727–738
36. Zelzer, E., Mamluk, R., Ferrara, N., Johnson, R. S., Schipani, E., and Olsen, B. R. (2004) *Development* **131,** 2161–2171
37. Bandyopadhyay, A., Tsuji, K., Cox, K., Harfe, B. D., Rosen, V., and Tabin, C. J. (2006) *PLoS Genet.* **2,** e216
38. Yayon, A., Klagsbrun, M., Esko, J. D., Leder, P., and Ornitz, D. M. (1991) *Cell* **64,** 841–848
39. Matsumoto, Y., Irie, F., Inatani, M., Tessier-Lavigne, M., and Yamaguchi, Y. (2007) *J. Neurosci.* **27,** 4342–4350
40. Paine-Saunders, S., Viviano, B. L., Economides, A. N., and Saunders, S. (2002) *J. Biol. Chem.* **277,** 2089–2096
41. Laufer, E., Nelson, C. E., Johnson, R. L., Morgan, B. A., and Tabin, C. (1994) *Cell* **79,** 993–1003
42. Hartmann, C., and Tabin, C. J. (2001) *Cell* **104,** 341–351
43. Guo, X., Day, T. F., Jiang, X., Garrett-Beal, L., Topol, L., and Yang, Y. (2004) *Genes Dev.* **18,** 2404–2417
44. Bradley, R. S., and Brown, A. M. (1990) *EMBO J.* **9,** 1569–1575
45. Dhoot, G. K., Gustafsson, M. K., Ai, X., Sun, W., Standiford, D. M., and Emerson, C. P., Jr. (2001) *Science* **293,** 1663–1666
46. Deirmengian, G. K., Hebela, N. M., O'Connell, M., Glaser, D. L., Shore, E. M., and Kaplan, F. S. (2008) *J. Bone Joint Surg. Am.* **90,** 366–374